Original Paper

Surface and depth profile analysis of insulating samples by TOF-SIMS

Olaf Anderson, Volker Scheumann, Uwe Rothhaar and Volker Rupertus
SCHOTT AG, Mainz (Germany)

The functionality of modern products made of glass, glass-ceramics, organics or other special materials is mainly dominated by the surface quality. A well defined lateral homogeneity of the surface stoichiometry is an important requirement for following added-value procedures, e.g. optical, mechanical or organic functional coatings.

As a characterization tool the time-of-flight secondary ion mass spectrometry (TOF-SIMS) provides analytical information about the chemical matrix in the surface near region with a lateral and depth resolution on the nanometer scale. Corrosion, contamination, interaction with the environment or diffusion of material components are typical phenomena, which can be studied in detail. The results lead to a deeper knowledge of the microscopic material behavior which is one of the basics for the understanding of complex processes in the field of development and production. Typical applications demonstrate the variety of operating a TOF-SIMS analytic tool, which is optimized for the investigation of electrically high insulating sample systems with various geometric appearance.

1. Introduction

Since the early 1980s, surface and thin film analysis has been applied in universal and industrial characterization laboratories [1 to 5]. Meanwhile many different techniques like X-ray induced photoelectron (XPS) or Auger electron spectroscopy (AES), high resolution transmission electron microscopy (TEM), scanning probe techniques (AFM, SNOM, STM), secondary ion or neutral mass spectrometry (SIMS, SNMS) as well as various scattering techniques based on ion, electron or photon impact have been developed and made commercially available [6].

But up to now the analysis of electrically high insulating samples is not yet state of the art. The available equipment can be adapted to insulating samples but in many cases the detected spectra or images are hampered by artifacts, which are induced by the measurement technique. Such effects are often originated by the charge transfer of the employed analytical techniques: electrons or ions, which hit or leave the sample surface, change the microscopic charge balance [7]. A second source of sample disturbance is the mean penetration or escape depth of the respective particles. Ions of a few keV primary energy are decelerated within a few nanometers and the charge transfer occurs within the near surface region, while electrons of the same energy reach a depth on the µm scale [8]. This simple example demonstrates the risks of "wrong" analysis parameters: In most cases a potential gradient is generated which leads to field induced diffusion of ionic species within the sample. Hence, the shape of the elemental depth profiles is influenced by the ratio of incoming and outgoing total amount of charge.

The key to avoiding or minimizing such effects is a maximum reduction of charge transfer to the sample. In that case TOF-SIMS is a proper choice, because this static SIMS version deals with primary ion current densities of a few pA/cm^2 far beyond typical current values of dynamic techniques by a factor of 10^3 to 10^6 [9].

Received 17 February 2004.
Presented in German at: 77th Annual Meeting of the German Society of Glass Technology in Leipzig (Germany) on 28 May 2003.

2. Experimental

The static TOF-SIMS measurements were performed with a TOF-SIMS IV-100 instrument (ION-TOF, Münster (Germany)). Spectra were acquired using a 15 keV $^{69}Ga^+$ primary ion beam. In order to achieve highest mass resolution ($m/\Delta m \approx 10\,000$) the spectra were detected in the so called "bunched mode" using a typical target current of the primary Ga^+ ions of about 2 pA.

To obtain spatially resolved ion images, Ga^+ ions were used with a kinetic energy of 25 keV and a total current below 1 pA. The ion gun was operated in extreme crossover mode, which results in a focus area with about 100 nm in diameter. Due to the low primary ion current, up to 100 images were accumulated to reach an adequate image contrast.

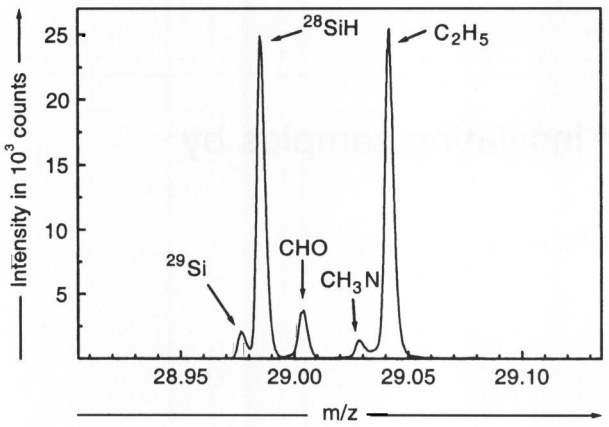

Figure 1. High mass resolution detail of signals around m/z = 29 of a glass surface spectrum.

For depth profiling the instrument is equipped with a low energy (0.25 to 2 keV) dual ion source column (DSC) including a Cs^+ liquid metal and an O_2^+ electron impact gun. The depth profile acquisitions were done in the "dual beam mode". In this mode the parameters of the analysis gun can be selected independently of the sputter gun parameters, which will be described in detail below. In order to suppress secondary ion signals originated nearby the crater edges the analysis beam was rastered over an area significantly smaller than the sputter crater size ("gating").

In all cases, charge compensation was achieved by applying low-energy electrons (20 eV) from a pulsed electron flood gun.

3. Resolution and detection limit

The mass resolution capability of "static" SIMS with $m/\Delta m$ > 8000 enables species with the same nominal masses to be resolved. For example ^{27}Al can be resolved from $^{11}B^{16}O$ or ^{56}Fe from $^{28}Si_2$. At high mass resolution most peaks from surface spectra are seen to be molecules, often with a hydrogen, hydrocarbon or oxygen component. An example is illustrated in figure 1 by the details around m/z = 29 of a mass spectrum from a glass surface. Besides the expected signal of ^{29}Si many fragments from surface contamination become visible in the spectra. They can be identified surely by a perfect mass scale calibration and matching with other signals.

Roughness and sample topography cause a significant reduction in the achievable mass resolution. This is partly due to different relative starting positions of secondary ions producing a spread in times to traverse the extraction gap. More important, the electrostatic field is reduced in dips and scratches by a screening effect. Therefore, it is recommended to use samples with flat and smooth surfaces and/or to reduce the analyzing area (e.g. (50 × 50) μm^2).

Insulating samples which dominate the majority of materials in the glass industry can generate special analysis problems. Unlike a conductor, the electric field used to extract ions, can penetrate into the bulk of an insulating material. Since the surface potential is no longer equal to the sample holder potential, the energy of the emitted secondary ions may move out of the energy acceptance of the analyzer and a lateral field gradient is introduced across the sample surface affecting the secondary ion trajectory and therefore the mass resolution due to their larger energy distribution. In the spectra, these ions show larger peak widths and high-mass tails which can overlap low intensity molecular fragments. This effect can be minimized by reduced sample thickness, lower extraction potentials or larger working distances.

TOF-SIMS has lower detection limits than TXRF (total reflection X-ray fluorescence), which is in widespread use today. In most cases the TOF-SIMS detection range is 10 to 10 000 times lower than that of TXRF. It can be as low as approximately 10^{-15} g/cm^2 (1 ppm of a molecule layer on the surface) or < 10^9 atoms/cm^2. The exact value depends on a lot of technical and physical/chemical parameters (measuring mode, analyzed area, ion beam, instrument, substrate and the kind of contamination or impurity). Values given in leaflets or other publications are approachable only under ideal conditions, e.g. on high-purity silicon or metal substrates.

In practice and under the realistic conditions of an industrial laboratory, the detection limits are much higher. In the following, such measurements for determining the detection limits will be described. Three reference glasses with certified concentrations of impurities were used: standard A: NIST SRM 612 [10], standard B: NIST SRM 614 [11] and standard C: BCR CRM 664 [12].

The measurements were performed with a Ga^+ ion beam in high current bunch mode with 15 keV energy and a current of 2 pA. The analyzed areas were (50 × 50) μm^2. In static mode the integration time was 60 s. Before analysis, the sample surfaces were cleaned for 1 min by sputtering with an O_2^+ ion beam (2 keV, 700 nA) or Cs^+ ion beam (2 keV, 140 nA) on areas of (300 × 300) μm^2, respectively. In dynamic mode the samples were sputtered for 2 s with O_2^+ and Cs^+, respectively, and analyzed for 1 s alternately with an integration time of 200 s. Mass spectra were collected with positive and negative polarity.

The results are collected in tables 1 and 2. The signals (peaks) in the mass spectra were inspected visually.

In some cases, the signal of the oxides (BO, SbO, ThO, UO) was taken, due to the higher intensity.

From the results depicted in table 1 the following conclusions can be drawn:

- The dynamic method (sputtering and analyzing alternatively) leads to a better detection capability in comparison to the static method (sputtering before analyzing).
- In positive polarity, most of the signals relevant for glass reveal higher intensities. Exceptions are F, Cl, S and BO, which can be detected only in negative polarity.
- Due to their higher intensities, it is recommended in some cases to detect the oxide fragments (BO, SbO, ThO, UO) instead of the atomic signals (B, Sb, Th, U).
- Sputtering or cleaning with oxygen results in higher intensities for positive polarity.
- Sputtering or cleaning with Cs^+ ions results in higher intensities for negative polarity.
- The signals of most of the elements are detectable in the concentration region of 30 to 50 ppm.
- The detection limit of most elements is a one-figure number in the ppm region.

Table 1. Qualitative detection sensitivity of typical glass ingredients

trace element	concentration in ppm	standard	static mode		dynamic mode	
			positive	negative	positive	negative
Ag	22	A	RL (O_2^+)	–	+ (O_2^+)	overlap (Cs^+)
Ag	0.42	B	–	–	–	–
As	6	C	overlap (O_2^+)	–	overlap (O_2^+)	–
Au	5	A	RL (O_2^+)	–	RL (O_2^+)	–
Au	0.5	B	–	–	–	–
B	32	A	++ (O_2^+), + (Cs^+)	BO: + (O_2^+, Cs^+)	+++ (O_2^+), + (Cs^+)	+ (Cs^+), BO: ++ (O_2^+)
B	1.3	B	+ (O_2^+, Cs^+)	BO: + (O_2^+, Cs^+)	++ (O_2^+), + (Cs^+)	+ (Cs^+), BO: ++ (O_2^+)
Ba	41	A	+ (O_2^+, Cs^+)	–	++ (O_2^+, Cs^+)	RL (Cs^+)
Ba	29	C	+ (O_2^+)	–	++ (O_2^+)	–
Cd	6	C	–	–	RL (O_2^+)	–
Cd	0.55	B	–	–	–	–
Ce	39	A	+ (O_2^+)	–	+ (O_2^+)	–
Gd	39	A	+ (O_2^+)	–	+ (O_2^+)	–
Cl	68	C	–	+++ (O_2^+, Cs^+)	Cs_2Cl: ++	+++ (O_2^+, Cs^+)
Co	35	A	+ (O_2^+)	–	++ (O_2^+)	CoO: RL
Co	3	C	RL (O_2^+)	–	+ (O_2^+)	–
Co	0.73	B	–	–	RL (O_2^+)	–
Cr	3	C	RL (O_2^+)	–	+ (O_2^+)	–
Cu	38	A	+ (O_2^+)	RL (O_2^+)	++ (O_2^+)	RL (O_2^+, Cs^+)
Cu	1.37	B	RL (O_2^+)	–	RL (O_2^+)	–
Dy	35	A	+ (O_2^+)	–	+ (O_2^+)	–
Er	39	A	+ (O_2^+)	–	+ (O_2^+)	–
Eu	36	A	+ (O_2^+)	–	+ (O_2^+)	–
Eu	0.99	B	–	–	RL (O_2^+)	–
F	88	C	RL (O_2^+)	+++ (O_2^+, Cs^+)	Cs_2F: + (Cs^+)	+++ (O_2^+, Cs^+)
Fe	51	A	++ (O_2^+), + (Cs^+)	–	+++ (O_2^+), ++ (Cs^+)	–
Fe	13.3	B	+ (O_2^+)	–	++ (O_2^+)	–
Ga	1.3	B	source	source	source	source
Gd	39	A	+ (O_2^+)	–	+ (O_2^+)	–
K	64	A	+++ (O_2^+, Cs^+)	+ (Cs^+)	+++ (O_2^+, Cs^+)	+ (Cs^+)
K	30	B	+++ (O_2^+, Cs^+)	+ (Cs^+)	+++ (O_2^+, Cs^+)	+ (Cs^+)
La	36	A	+ (O_2^+)	–	++ (O_2^+)	–
La	0.83	B	RL (O_2^+)	–	+ (O_2^+)	–
Mn	40	A	+ (O_2^+, Cs^+)	–	++ (O_2^+, Cs^+)	–
Nd	36	A	+ (O_2^+)	–	+ (O_2^+)	–
Ni	39	A	+ (O_2^+)	–	++ (O_2^+)	–
Ni	0.95	B	–	–	RL (O_2^+)	–
Pb	53	C	+ (O_2^+)	–	+ (O_2^+)	–
Pb	39	A	+ (O_2^+)	–	+ (O_2^+)	–
Pb	2.32	B	RL (O_2^+)	–	RL (O_2^+)	–
Rb	31	A	+ (O_2^+, Cs^+)	–	++ (O_2^+), + (Cs^+)	–
Rb	0.85	B	RL (O_2^+)	–	+ (O_2^+)	–
S	4000	C	+ (O_2^+)	+++(O_2^+, Cs^+)	RL (Cs^+)	+++ (O_2^+, Cs^+)
Sb	24	C	SbO: RL (O_2^+)	–	+ (O_2^+)	–
Sb	1.06	B	–	–	–	–
Sc	0.59	B	–	–	RL (O_2^+)	–
Se	9	C	–	–	–	–
Sm	39	A	+ (O_2^+)	–	+ (O_2^+)	–
Sr	78	A	+++ (O_2^+)	–	+++ (O_2^+), ++ (Cs^+)	–
Sr	45.8	B	+++ (O_2^+)	–	++ (O_2^+), + (Cs^+)	–
Th	38	A	ThO: + (O_2^+)	–	ThO: + (O_2^+)	–
Th	0.75	B	–	–	–	–
Ti	50	A	++ (O_2^+), + (Cs^+)	–	+++ (O_2^+), ++ (Cs^+)	–
Ti	3.1	B	+ (O_2^+)	–	++ (O_2^+)	–
Tl	16	A	RL (O_2^+)	–	RL (O_2^+)	–
Tl	0.27	B	–	–	–	–
U	37	A	UO: + (O_2^+)	–	UO: + (O_2^+)	–
U	0.82	B	UO: RL (O_2^+)	–	UO: RL (O_2^+)	–
Yb	42	A	+ (O_2^+)	–	+ (O_2^+)	–

Note: +++: excellent signals with very high intensity; ++: very good signals with high intensity; +: good signals with adequate intensity; RL: impurity detectable but signal near recognition limit; –: not detectable.

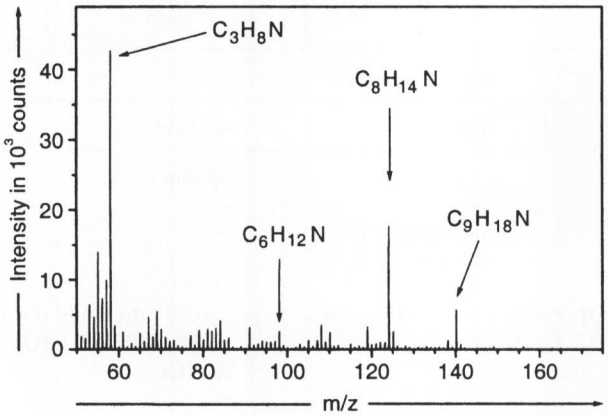

Figure 2. Positive TOF-SIMS spectrum of a glass slide after storage for 10 d at 60 °C in a plastic box.

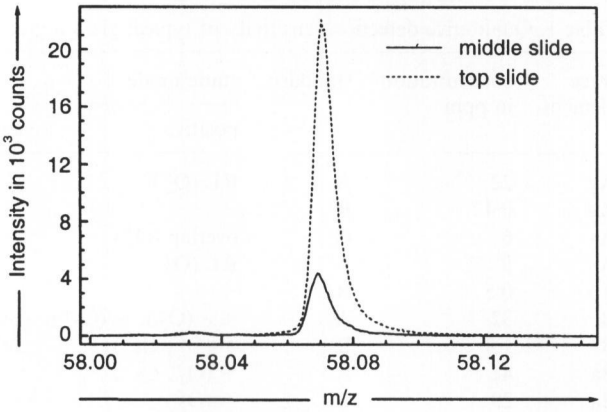

Figure 3. Overlay spectra at mass 58 indicating UV stabilizer.

- By using Cs^+ clusters (Cs_2F, Cs_2Cl) it becomes possible to measure the signals of Cl and F in positive polarity, too. This is also valid for S, but the overlap of the Cs_2S signal and the Cs_2O_2 signal prevents its utilization.
- The detection limit depends on integration time, underground signal height and overlapping neighbour peaks.

4. Surface analysis

4.1 Silane coated glass slides

Analyses of DNA chips play a key role in pharmaceutical research and development. They make it possible to carry out gene expression analyses of healthy and diseased tissue samples at high throughput rates. The more reliable the respective results are, the more accurate is the opportunity for the development of appropriate drugs. DNA chips are based on silane coated glass slides. The homogeneity and reproducibility of the silane film is one of the key factors for the performance of the entire system. Hence, the coated slides are packed in boxes to protect the activated surface from light and maintain a stable storage environment. If plastic boxes are used, the surface could be contaminated by outgassing additives like W-stabilizers or plasticizers. Figure 2 shows a TOF-SIMS spectrum of a glass slide after a storage time of 10 d at 60 °C in a plastic box. The appearance of mass 58, 98, 124 and 140 indicates the presence of typical UV stabilizers on the surface.

Figure 3 displays an overlay of two detail spectra in the vicinity of mass 58 which is a characteristic signal for UV stabilizer. It is clearly shown that the top slide, facing the plastic box wall, is much more contaminated than the slide positioned in the middle of the container.

This example demonstrates in an impressive way the capability of TOF-SIMS measurements to identify contamination at very low levels. Regarding these results it was possible to find a suitable packaging material that fulfills the special product requirements.

4.2 Image analysis ("mapping") of contaminated surfaces

The increasing performance of recent devices based on glass substrates lowers the tolerance of contamination that might be difficult to detect with traditional inspection and analysis techniques.

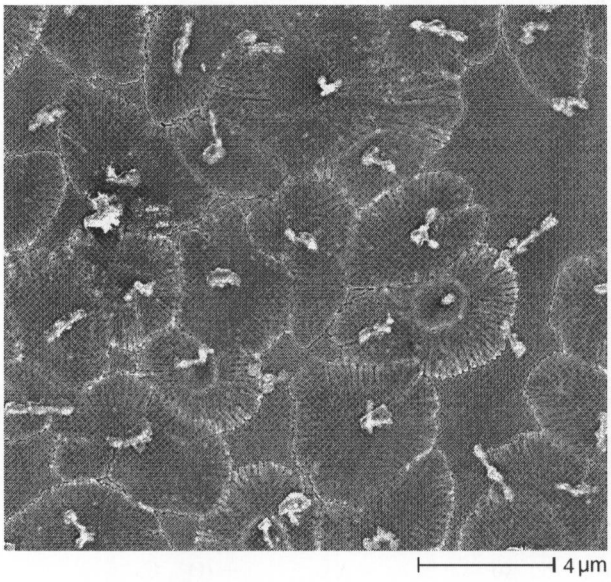

Figure 4. SEM image of ceramization seeds on LAS glass.

Image analysis by TOF-SIMS provides sensitive detection and high lateral resolution (less than 200 nm) of both elemental and molecular contamination that may originate from environmental sources or from cleaning processes.

Compared to scanning electron microscopy (SEM) in combination with energy dispersive X-ray spectroscopy (EDX), where the information depth is in the range of 1 µm, TOF-SIMS has a sampling depth of only 1 to 2 monolayers.

Images of the surface are generated by rastering an ion beam over a chosen area. The resulting secondary ion images or ion beam induced secondary electron images can be used to accurately locate the feature of interest with the subsequent acquisition of a mass spectrum from the user-selected area. As a result TOF-SIMS allows identification of the organic and inorganic composition including boron and lithium of specific features on a sample, such as defects, stains or particles.

The SEM micrograph in figure 4 shows a top view of a LAS glass with typical structures of surface crystallization. In combination with the elemental distribution derived from

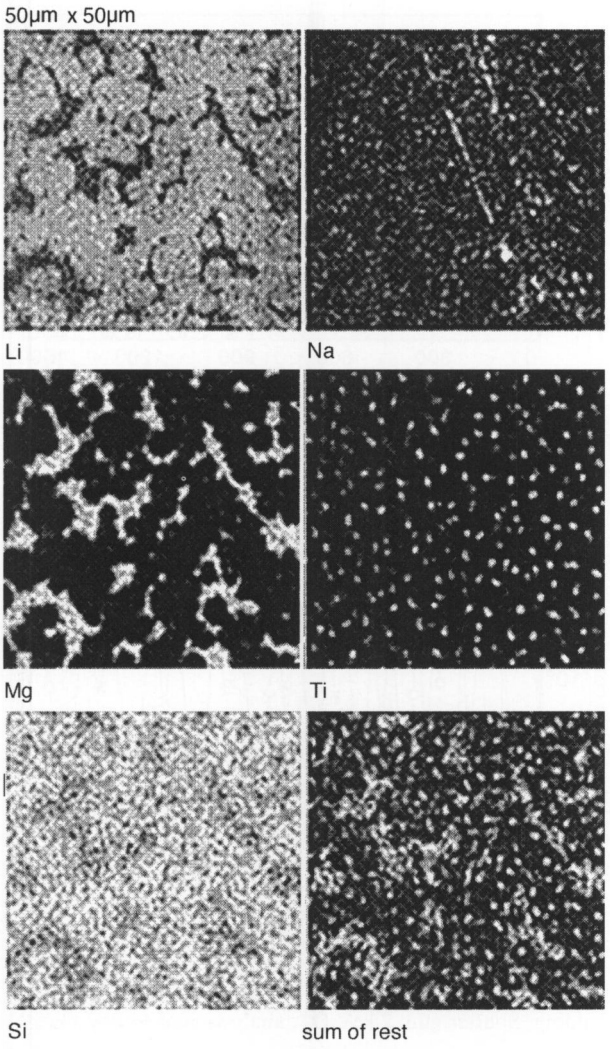

Figure 5. TOF-SIMS images ((50 × 50) µm²) of the elemental distribution of a LAS glass with surface crystallization.

TOF-SIMS images (figure 5) the presence of titanium seeds surrounded by lithium rich regions becomes quite evident. In that case beginning surface crystallization in an early state becomes visible.

5. Depth profile analysis

Depth profiling by SIMS employing a DC ion beam and a quadrupole or magnetic sector mass spectrometer is very commonly used, especially in the semiconductor industry. The sample is continuously eroded by ion bombardment, while the intensities of the ions of interest are detected sequentially. In TOF-SIMS, all elements are acquired simultaneously. Using the so-called dual beam technique for depth profiling, the sputtering process is separated from the detection phase. This kind of decoupling provides a number of advantages, in particular for the analysis of insulators. During the erosion phase, a low-energy, high-current-density electron flooding is used to minimize the positive charging-up of the sample. Compared with the current density of the sputtering ion beam, the current density in the subsequent analyzing phase is very low (static conditions).

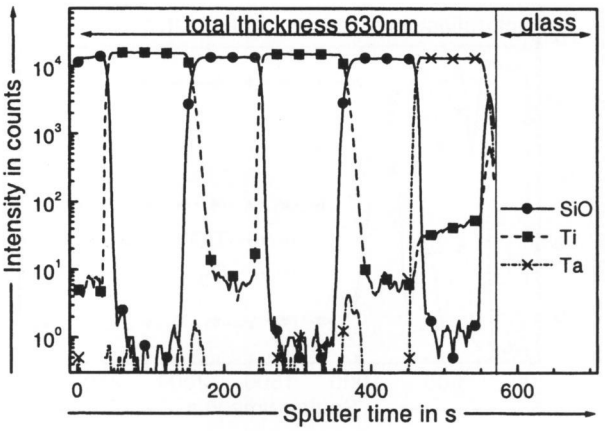

Figure 6. Sputter time profile of an optical multilayer system on flat glass.

Therefore, the surface modification (atomic mixing etc.) as well as the depth resolution are given mainly by the energy and the species of the sputtering ions (e.g. Ar^+, O_2^+, Cs^+) [13 and 14]. Additionally, sample charging becomes easier to handle. Up to the last years one big disadvantage of TOF-SIMS depth profiling was the relatively long measuring time due to the alternating erosion and analysis cycles. Today, sputtering ion sources with high ion current densities are available which enable sufficiently high erosion rates (e.g. 3 µm/h). To demonstrate the capability of this technique, four examples of depth profiling insulating material are depicted below.

5.1 Optical filter system on flat glass

Figure 6 shows a positive SIMS sputter time profile of an SiO_X, TiO_Y, TaO_Z multilayer structure (six single layers) with a total thickness of approximately 630 nm on glass. The measurement was carried out using a 2 keV O_2^+ beam for sputtering (area (300 × 300) µm²) and 15 keV Ga^+ ions for acquisition (area (50 × 50) µm²). As can be readily seen from the time axis in figure 6, the overall erosion rate exceeds 1 nm/s, which means 3.6 µm/h. Taking into account the additional time for the analyzing cycles, the total profiling process took only 20 min. On the other hand the profiles of the multilayer system show an excellent depth resolution and an adequate dynamic range (3 to 4 orders of magnitude) throughout the entire structure. This combination of technical performance and throughput speed demonstrates the effectivity, which is an important factor especially for investigations within industrial environment.

5.2 Combined anti-reflective and anti-scratch coating on PMMA

The depth profile of a functional coating (anti-reflective + anti-scratch) on polymethyl methacrylate (PMMA) employing 2 keV Cs^+ for sputter removal and monitoring the negative ions is depicted in figure 7. Again the analysis was performed using a rastered 15 keV Ga^+ ion beam ((50 × 50) µm²). Besides the insulating character of the polymer substrate, additional care must be taken for the ion-bom-

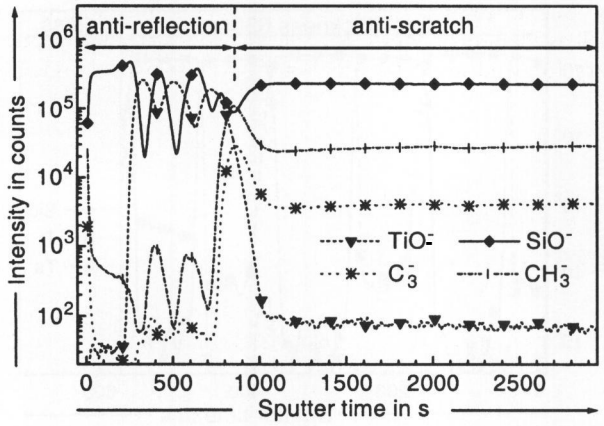

Figure 7. SIMS intensity versus sputter time profile of an anti-reflective and anti-scratch coating on a PMMA substrate.

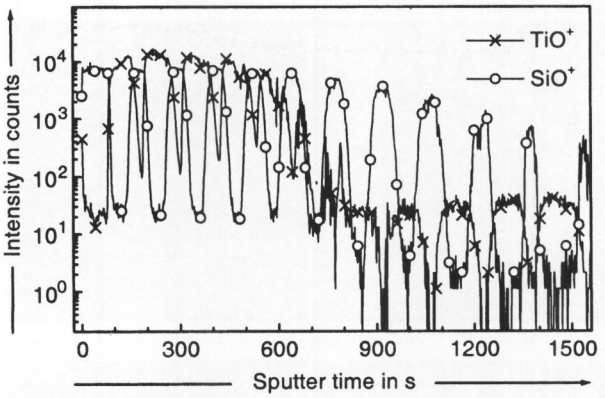

Figure 8. Depth profile of SiO_2 / TiO_2 multilayers on glass before grinding. Sputter gun: 2 keV O_2^+, analysis gun: 15 keV Ga^+.

bardment-induced temperature rise during the measurement, because PMMA tends to soften above 80 °C. To overcome the latter problem, short erosion cycles and increased pause periods between sputtering and acquisition were chosen. The reflectivity is reduced by an alternating system of SiO_X and TiO_Y layers whereas the anti-scratch coating consists of $SiO_XC_YH_Z$ material as can be seen from the signal profile in figure 7. The appropriate deposition was performed in-situ with the plasma induced chemical vapour deposition (PICVD) technique using hexametyldisiloxane (HMDSO), titanium chloride ($TiCl_4$) and oxygen as precursor gases. A detailed process description is given elsewhere [15].

5.3 Cold mirror on glass

A so called "cold mirror" multilayer coating reflects light in the visible wavelength range and transmits in the IR region. For this type of coating many applications are known. In the example described here, the coating consists of highly insulating layers of SiO_2 and TiO_2 on a glass substrate. During the depth profiling analyses the bombardment and emission of ions and electrons is changing the surface potential. As a consequence of this charge transfer the energy distribution of secondary ions and collection efficiency will be altered. In order to eliminate the charge accumulation, low energy electrons are flooded over the sample between two subsequent primary ion pulses. Although this charge compensation is usually sufficient, high sputter ion currents, a large number of layers (up to 60) and extremely low conductivity require a good electrical contact with the sample holder in order to avoid surface potential changes. Figure 8 shows a depth profile of a multilayer on a curved glass substrate. During the measurement the sample was clamped towards the backside of the sample holder. Due to the given geometric curvature of the glass substrate, only three sharp edges of the sample came in contact with the sample holder. The small contact area between the sample and sample holder results in unstable charge build-up conditions and therefore in decreasing collection efficiency over time. In order to increase the contact area and minimize the sputter crater to sample holder distance, the sharp edges have been removed by grinding. In addition with the flux of low energy electrons the larger contact area leads to the profile

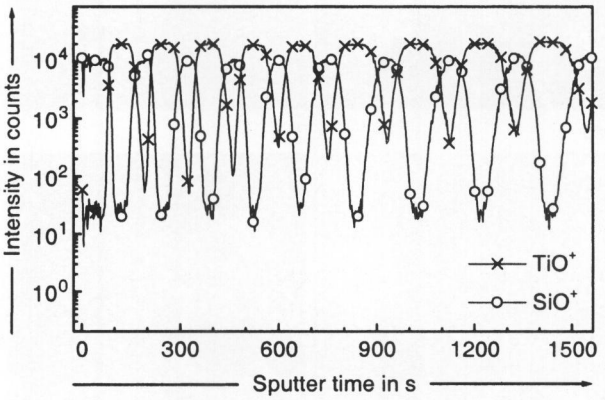

Figure 9. Depth profile of SiO_2 / TiO_2 multilayers on glass after grinding. Sputter gun: 2 keV O_2^+, analysis gun: 15 keV Ga^+.

shown in figure 9. This example shows that an optimized sample preparation can improve the depth profiling of thick insulating systems.

5.4 Optical fiber

An increasing amount of optical products is based on glass fibers. Every optical fiber consists of a core with a high refractive index material and a cladding with a lower refractive index. Light rays that enter the fiber are guided along the core by total internal reflections at the core/clad interface, the light rays follow all the bends in the fiber and exit the fiber at its end. Bundles of optical fibers are combined with appropriate end caps and protective sheathing to form light guides. In recent years fibers can especially be found in various automotive applications. Apart from the safety advantage achieved through the use of cold light for lighting applications, the light source is better accessible and in particular such a system offers design opportunities. Recently optical data transmission networks have also successfully found their way into vehicles. In this example TOF-SIMS was used to discover the effects of high humidity exposure onto optical transmission. Due to the small fiber diameter of 50 µm the surface was heavily curved. For the sample preparation an indium foil was employed. In order to reach high depth resolution on the curved fiber an analy-

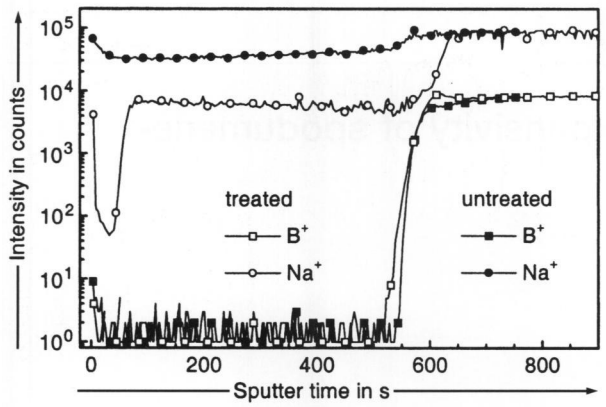

Figure 10. Overlay of two depth profiles of single fibers with and without humidity exposure. Sputter gun: 2 keV O_2^+, analysis gun: 15 keV Ga^+.

sis area of only (10 × 10) μm^2 was chosen. Figure 10 shows an overlay of the depth profiles from the humidity treated fiber and the untreated one. After the climate test a strong depletion of sodium in the cladding region is observed leading to a decrease in optical transmission.

6. Conclusion

The results demonstrate that:

a) TOF-SIMS surface and depth profile analysis has grown to a powerful tool for qualitative elemental analysis of glass samples of any kind.

b) The detection limits of typical glass components and impurities are mostly in the lowest ppm region.

c) The combination with an imaging device leads to additional lateral information and provides similar to SEM/EDX visual and chemical information, but only of the topmost atom layer.

d) The small diameter of the analyzing ion beam results in 100 nm lateral resolution and delivers accurate analysis of critical geometric curvatures even in the depth profile mode.

All these features lead nowadays to information of the chemical composition of the topmost monolayers and the elemental distribution in the surface near region, even in high insulating sample systems.

Contact:

Dr. O. Anderson
SCHOTT AG
Hattenbergstraße 10
D-55122 Mainz
E-mail: Olaf.Anderson@schott.com

But up to now the appropriate sample preparation as well as the proper choice of analyzing parameters are necessary to avoid artifacts, which are not automatically identified.

7. References

[1] Briggs, D.; Seah, M. P.: Practical surface analysis. Vol. 1 and 2. Chichester: Wiley, 1996.
[2] Daris, L.; MacDonald, N.; Palmberg, P. et al.: Handbook of Auger electron spectroscopy. Physical Electronics Division, Eden Prairie, MN, 1978.
[3] Benninghoven, A.; Ruedenauer, F. G.; Werner, H. W.: Secondary ion mass spectrometry. New York: Wiley, 1987.
[4] Behrisch, R.: Sputtering by particle bombardment. I. Heidelberg et al.: Berlin et al.: Springer, 1983.
[5] Behrisch, R.; Wittmark, K.: Sputtering by particle bombardment. III. Berlin et al.: Springer, 1991.
[6] Bubert, H.; Jenett, H.: Surface and thin film analysis. Weinheim: Wiley-VCH, 2002.
[7] Rupertus, V.; Martin, D.; Rothhaar, U. et al.: Steuerung und Optimierung teilchenstrahlinduzierter Oberflächenprozesse von Isolatorwerkstoffen. In: Proc. Statusseminar Dünnschichttechnologien. Düsseldorf: VDI-TZ Phys. Technol., 1992. P. 791.
[8] Eckstein, W.: Computer simulation of ion-solid interactions. Berlin et al.: Springer, 1991.
[9] Vickerman, J. C.; Briggs, D.: TOF-SIMS: Surface analysis by mass spectrometry. Chichester: IMPublications, 2001.
[10] Certificate of Analysis, NIST Standard Reference Material 612, http://patapsco.nist.gov/srmcatalog/certificates/view_cert2gif.cfm?certificate=612.
[11] Certificate of Analysis, NIST Standard Reference Material 614, http://patapsco.nist.gov/srmcatalog/certificates/view_cert2gif.cfm?certificate=614.
[12] European Commission, bcr information. Report EUR 18852 EN (1999).
[13] Iltgen, K.; Benninghoven, A.; Niehuis, E.: Profiling with optimized depth resolution. In: Gillen, G.; Lareau, R.; Bennett, J. et al. (eds.): Secondary ion mass spectrometry (SIMS XI). Chichester: Wiley, 1998. P. 367.
[14] Iltgen, K.; Bendel, C.; Benninghoven A. et al.: Optimized time-of-flight secondary ion mass spectroscopy depth profiling with dual beam technique. J. Vac. Sci. Technol. **A 15** (1997) no. 3, pp. 460–464.
[15] Kuhr, M.; Bauer, S.; Rothhaar, U. et al.: Coatings on plastics with the PICVD technology. Thin Solid Films **442** (2003) pp. 107–116.

E404P002